LUND UNIVERSITY
Faculty of Science

Design of solvent vapor annealing tool and study of kinetics of self-assembly block copolymers for nano-lithography

Chujun Wang

Thesis submitted for the degree of Master of Science
Project duration: 4 months

Supervised by Ivan Maximov

Department of Physics
Division of Solid State Physics
June 2020

Abstract

Block copolymer lithography is a very promising candidate for nanoscale fabrication and is economically viable. It provides a high resolution, inexpensive, and straightforward approach to nano-size patterning. In this thesis, fundamental concepts and theories of block copolymer lithography are introduced. A well-controlled dynamic solvent vapor annealing chamber is built, and the best annealing condition using this chamber is investigated. Two changed parameters in this thesis are annealing time and initial film thickness. By using atomic force microscopy and other characterization methods, self-assembly structures of PS-*b*-P4VP films before and after solvent annealing with Tetrahydrofuran are studied. The best arrangement of hexagonally packed vertical cylinders is obtained after 60 min annealing with initial polymer film thickness around 50-57 nm and reaches its equilibrium pitch of 58 nm. This thesis also contains the study of kinetics of the self-organization process of block copolymer films during annealing.

Contents

Acronyms

IC	Integrated Circuit
UV	Ultraviolet
EUV	Extreme Ultraviolet
EBL	Electron Beam Lithography
NIL	Nanoimprint Lithography
BCP	Block Copolymer
SVA	Solvent Vapor Annealing
PS-*b*-P4VP	Poly(Styrene)-block-Poly(4-Vinylpyridine)
THF	Tetrahydrofuran
AFM	Atomic Force Microscopy
ALD	Atomic Layer Deposition
sSVA	Static Solvent Vapor Annealing
dSVA	Dynamic Solvent Vapor Annealing
MFC	Mass Flow Controller
SEM	Scanning Electron Microscopy
IPA	Isopropanol

Chapter 1

Introduction and Background

1.1 Motivation and Outline

Since the inception of the integrated circuit (IC), which packs transistors and other functional electronic components in one device, it has been developing rapidly and became the cornerstone of the modern information society. In order to sustain the evolution of Moore's law, patterning of silicon structures with continually reduced feature sizes has been the main path of semiconductor manufacturing. Lithography has been one of the core technologies to promote the design of advanced integrated circuits and their device replacement. Development of lithographic techniques with increased resolution has been in decades the driving force in emergence of new generations of integrated circuits.

Photolithography has been the most commonly used method of making planar microstructures. In optical lithography, a thin layer of a polymer material called photoresist is deposited on a flat substrate surface. The ultraviolet (UV) light is focused onto the photoresist through a mask, and a desired pattern is created on the substrate (1). However, the resolution of optical lithography is limited by the wavelength of the light source and diffraction. Pattern sizes have shrunk and are now below the wavelength of light used (193 nm) to pattern them (2). One way to improve the resolution by using smaller wavelength light is extreme ultraviolet lithography (EUV) with extreme UV light at 13 nm wavelength. However, it currently encounters a host of technological challenges, such as EUV source power output, the availability of defect-free masks and EUV's considerable cost (3), that prevents it from being widely used.

Electron beam lithography (EBL) is also an essential and versatile technology used in nanofabrication. Electrons work very much like photons to interact with photoresist. EBL uses high-energy electrons with corresponding ultra-short wavelengths so the EBL resolution is limited by other factors, such as the proximity effect and the beam spot size. Besides, EBL is a very flexible nanofabrication method compared to photolithography due to the fine electron beam enabled by electron optics (1). However, as mentioned above, the proximity effect, which results from interaction of electrons with the substrate, severely limits resolution and pattern density of EBL-defined structures, and represents one of the major bottlenecks of EBL together with very low throughput of this technique. Another alternative sub-100 nm patterning method is nanoimprint lithography (NIL), which can obtain high-resolution and large-area patterns. In the nanoimprint, a pattern is transferred by a mechanical contact between a hard stamp and soft polymer layer. In this high-throughput approach there are no diffraction limitations, so the NIL resolution can be as high as a few nanometers, but mechanical contact during the imprint puts high demands to the stamp quality.

Conventional high-resolution lithographic techniques discussed above rely on a "top-down" approach to make nanostructures. This approach is either flexible but slow and expensive (EBL), or more suitable for replication of a fixed pattern (NIL), so other methods of patterning are being developed. One such method is the self-assembly of block copolymers (BCP) that provides an inexpensive and straightforward approach to nano-size patterning and can be used in lithography and with other nanofabrication methods. It can reach sub-10 nm resolution over large areas of several square centimeters and is suitable for regular arrays of nanostructures, such as dots or lines. The BCP-approach is based on self-organization of block co-polymers in regular structures to minimize the free energy of the system. However, the self-assembled structures may not be perfectly well-organized or may not form the preferred structure for further use. In order to control the self-assembly, an additional annealing step is required, in which the elevated temperature provides sufficient thermal energy to re-arrange the polymer molecules. Very often, the annealing is performed in a suitable vapor atmosphere, using so-called solvent vapor annealing (SVA).

This project focuses mainly on two parts: firstly, design and building of a simple SVA chamber to provide a controllable environment for the annealing of BCPs and secondly to investigate the optimized annealing conditions of the dynamic solvent vapor annealing setups and study of self-assembly kinetics of Poly(Styrene)-block-Poly(4-Vinylpyridine) (PS-*b*-P4VP) films on Si substrate. The SVA chamber should allow annealing of the BCP films in a stable vapor atmosphere and prevent negative effects of ambient conditions such as variations of temperature and humidity. The kinetics of the self-organization process of the BCP films should also be studied, using both in-situ measurements and high-resolution microscopy techniques such as Atomic Force Microscopy (AFM). Some of the annealing process parameters, such as annealing time and film thickness, will be studied to relate their effects on the morphology of the obtained BCP films.

In chapter 2, the design of the experiment and characterization methodology will be described. The detailed design of a dynamic solvent vapor annealing chamber and the function of each part will be discussed. An annealing setup based on the chamber is also introduced. Besides, it also involves the fundamental theories and applications of characterization methods used in this project. Chapters 3 and 4 mainly discuss two parameters that influence the morphology of BCP films during annealing, annealing time, and initial film thickness in chapters 3 and 4, respectively. Conditions and procedures of the experiment and discussions of the results are also involved in these two chapters. The last chapter, chapter 5, is a summary of the thesis and includes some possible further work based on this project.

1.2 Basics of Block Copolymers

Block copolymers (BCP) are polymer materials where different polymer segments are covalently bonded to each other. Under certain conditions, they can generate regular patterns with periods ranging from 5 to 100 nm. Due to those properties of BCPs, they can be used in

nanofabrication. BCP films can be easily prepared by spin-coating a copolymer layer on the substrate and then annealing to arrange themselves to useful and periodic patterns. Among all kinds of block copolymers, diblock copolymers are the simplest and most commonly used ones. Diblock copolymers are two chemically distinct polymer chains connected linearly with a covalent bond (4). Due to their different chemical properties, BCP blocks interact with each other and undergo phase segregation at a temperature lower than their order-disorder transition temperature (5).

The significant factors influencing the type of self-assembly are the Flory-Huggins segmental interaction parameter χ, degree of polymerization N, and the volume fraction of one block *f* (6). The theory of BCP self-assembly is well-developed and successfully predicts the phase diagram of the equilibrium morphology of BCP bulk melts, as shown in figure 1-1. The shape of domains is determined by volume fraction of the components, and the size of domains is dictated by the molecular weight of polymers. χ is proportional to the strength of interactions between different blocks (7) and is temperature influenced as $\chi \sim T^{-1}$. The arrangements of the domains are similar to the structures formed in lipid and micellar systems and consist of several different morphologies. However, not all of these morphologies are capable of being used in nano-lithography applications. Among these morphologies, the hexagonally packed vertical cylinders where one block forms cylinders embedded by the other block is the one that fulfills our requirements, which can be used in further nanofabrication, like nanowire growth. So, in order to accurately define and control the structural orientation of these films, the surface energy must be well modified.

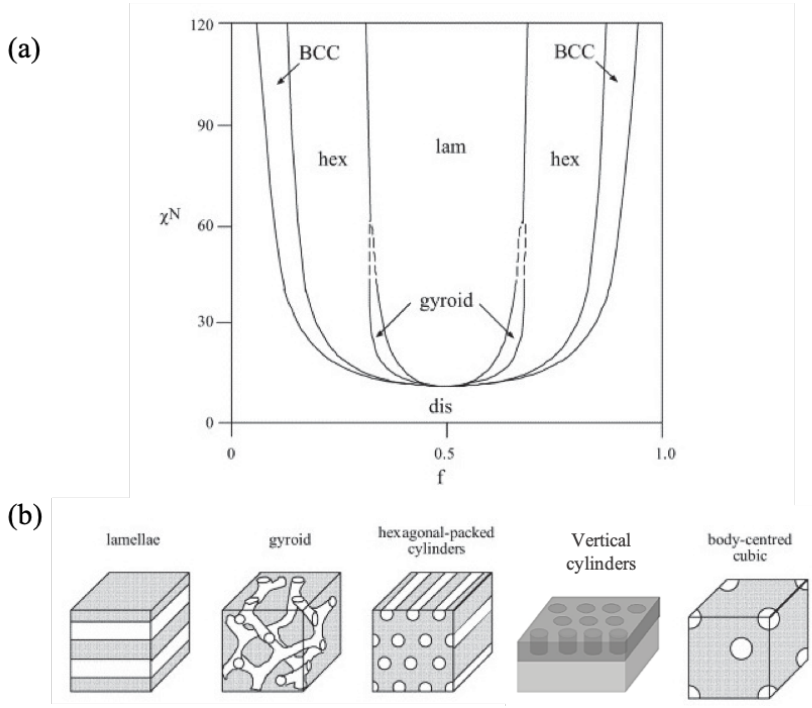

Figure 1-1 (a) Phase diagram of a diblock copolymer; (b) Related morphologies. Regions of stability of disordered (dis), lamellar (lam), gyroid, hexagonal (hex), vertical cylinders (3), and body-centered cubic (BCC) phases are indicated (7).

The suitable material system for nanofabrication is polymers with high χ because it is easier to control the relative volume of the polymer segments and get small interfacial widths for minimal line edge roughness (8), also the BCPs with high χ result in small domain structures. The orientation of BCP domains is also critical for BCP applications in nanofabrication (7) because by combining with a selective modification of one block array, the pattern could transfer to the substrate. Such modification could be dry etching via evaporated metal etch mask on the BCP template (9), or so-called surface reconstruction using a solvent selective to one of the blocks. For the dry etching method, one block on polymer array is evaporated and lifted-off to leave the nanodot structure used for further fabrication such as atomic layer deposition (ALD). Figure 1-2 shows one example of such method. For the surface reconstruction process, a BCP film with cavities will remain after the evaporation of the solvent, and the remaining surface structure is suitable for lithography application or for high-density III-V nanowire growth used in vertical nanowire transistors (10, 11).

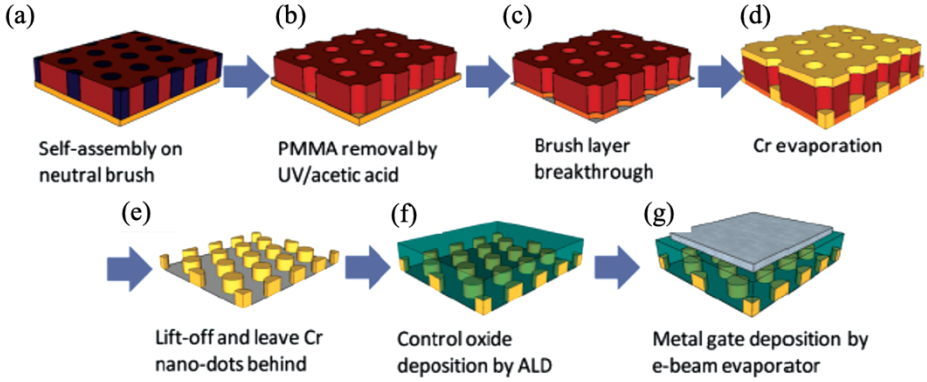

Figure 1-2 Schematics of process flow for metal nanodot memory device using PS-*b*-PMMA and Cr evaporation (9).

1.3 Annealing Methods

1.3.1 Thermal Annealing

As mentioned above, the initial organizations formed by block copolymers themselves after for example spin-coating, are usually disordered and undesired for further application. An additional annealing step should be used to control the self-assembly process and remove defects. Thermal annealing is implemented by raising the temperature of the system near the glass transition temperature to allow kinetically trapped polymers to diffuse towards a state with equilibrium energy. In a typical thermal annealing process, BCP thin films are simply heated above its glass transition temperature and held at elevated temperature for a specific time, then cooled down to room temperature (7). However, the high χ BCP materials that are of biggest interest for nanofabrication, have a rather low diffusivity and need a long annealing time and high annealing temperature. These conditions are sometimes difficult to reach due to the risk of a thermal degradation.

1.3.2 Solvent Vapor Annealing

Solvent vapor annealing (SVA) is an alternative method for BCP films that overcomes the disadvantages of thermal annealing. It has proven to be a powerful technique for BCP films to obtain different equilibrium structures with low defect concentration. In SVA, block polymer thin films are exposed to solvent vapors with temperatures typically below the glass transition temperature of both blocks. The polymer absorbs solvent vapor and forms a swollen and mobile polymer film on top of the substrate (6). By absorbing the solvent vapor, the volume fraction changes, leading to the change in morphology. It also changes the polymer concentration in the film, resulting in a reduction of the effective interaction parameter and an improvement in the kinetic pathway for morphology evolution (8). Another SVA step is the drying step, during which the solvent evaporates from the BCP films and determines the domain structures. The advantage of this process is the significantly reduced annealing temperature and the possibility to alter morphology by tuning solvent selectivity compared to thermal annealing and the possibility to anneal polymers with the order-disorder transition temperature higher than the degradation temperature.

There are several different ways of processing solvent vapor annealing. Perhaps the simplest and widely implemented one is static SVA (sSVA) (8), which simply places the BCP film and a volume of liquid solvent in a sealed, temperature-controlled environment. However, solvent saturation conditions using sSVA setups are typically poorly controlled and easily influenced by ambient conditions. Furthermore, vapor leakage could also appear and change the solvent vapor pressure during annealing, which will change the final morphology and cause defects. An improved way of such a method is using a chamber with inlet and outlet gas lines for solvent vapor. In this SVA method, the solvent is carried in the vapor phase by a carrier gas into the chamber, and both the absolute pressure and vapor pressure inside the chamber are well-controlled (12).

Another foremost condition for the SVA setup is the selection of the solvent. The most effective solvent for SVA of block polymers is neutral or only slightly selective for one of the blocks (6). The Hildebrand solubility parameter can determine the selectivity, and the solvent has selectivity only to polymers having very similar Hildebrand solubility parameters (13). The final morphology of the self-assembly is also related to the solvent selection and the solvent selectivity to the polymers.

1.4 Block Copolymer System Used in This Project

In this project, Poly(Styrene)-block-Poly(4-Vinylpyridine) (PS-*b*-P4VP, 50-*b*-17 kg/ mol) with a polydispersity index of 1.15 purchased from Polymer Source Inc. (Canada) is used as the block copolymer and tetrahydrofuran (THF) as the solvent. The Hildebrand solubility parameters of THF, PS, and P4VP are 18.5, 18.3, and of 22.2 $MPa^{1/2}$, respectively (14). According to previous section solvent has selectivity only to polymers having very similar Hildebrand solubility parameters, so THF has the selectivity to PS and no selectivity to P4VP.

There are several advantages of using PS-*b*-P4VP, in BCP based nanofabrication, compared to other BCPs. Firstly, it has high χ, which enables patterns with small periodicities. Besides, the P4VP interacts easily with metal or small molecules, forming possible routes for functionalization, the inclusion of nanoparticles (15), or increased etch selectivity. High χ BCPs are favorable to high-density pattern applications and could increase the resolution for further application. For a PS-*b*-P4VP film with a similar proportion of PS and P4VP, it is more spontaneously to form a lamella structure and is difficult to change morphology after annealing with THF (13, 16), which is not preferred for our project. By increasing the ratio of PS, vertical cylinder structures can be formed before annealing. However, if the ratio difference between the two polymers is too large, the spherical structure will be formed (17). Therefore, in order to have a hexagonally packed cylinder structure, a proper polymer ratio should be chosen, and in this project we are using a polymer with an approximately 0.25 volume fraction of P4VP.

1.5 Summary

This chapter introduces some background theories and motivation for the project. Block copolymer lithography is a very promising candidate for nanoscale fabrications and is economically viable. The concepts, applications, and important parameters of BCP are introduced. Furthermore, in order to have a good control of BCP self-assembly, additional annealing methods are used, and two popular annealing methods are shown in this chapter. More details of solvent vapor annealing are discussed because it is the method used in this project. The contents of this thesis is also involved in this chapter.

Chapter 2

Experiment Design and Methodology

2.1 Dynamic Solvent Vapor Annealing Chamber

The basic solvent vapor annealing setup – static solvent vapor annealing (sSVA), used in the previous experiments consists of just two beakers. A larger beaker that contains the solvent mixture is sealed by laboratory films and tapes and placed at room temperature during the annealing. The samples are not immersed in the liquid but placed in a smaller beaker inside the sealed container. At the end of the annealing time, the samples are removed from the larger beaker and left in ambient conditions for 10 minutes. This sSVA setup is easy and simple to operate. However, it has poor control of the annealing condition, such as the humidity, ambient temperature, and the solvent vapor evaporate rate, which could hinder the repeatability and lead to unwanted defects. Figure 2-1 is the illustration of this sSVA setup used for previous experiments in our group.

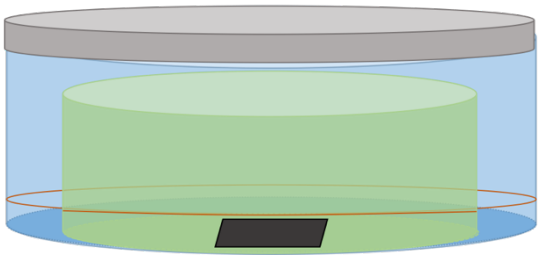

Figure 2-1 The illustration of a simple sSVA setup. The blue and green column illustrate the larger and smaller beaker. The sample is depicted in black, with the liquid solvent surface shown in red.

In order to overcome the disadvantages of the sSVA process, a dynamic solvent vapor annealing chamber (dSVA), which provides a controllable environment for the annealing of the BCPs, is built. The primary purpose of this device is to create a stable solvent vapor atmosphere with one or more solvents for the thin polymer film placed in it. This chamber should be able to maintain constant humidity, temperature and thus the controllable solvent vapor evaporation rate during the annealing. By using this chamber, a significant improvement for the reproducibility from the previous experimental results can be reached. This system takes advantage of steady-state vapor flows formed in it to fasten the annealing process and to create more reproducible experimental conditions for every experiment. Besides, the chamber creates an isolated environment, which reduces the interruptions from the ambient conditions. Furthermore, the chamber is also designed to have good control of the pressure and temperature and allow in-situ optical measurements during the annealing process.

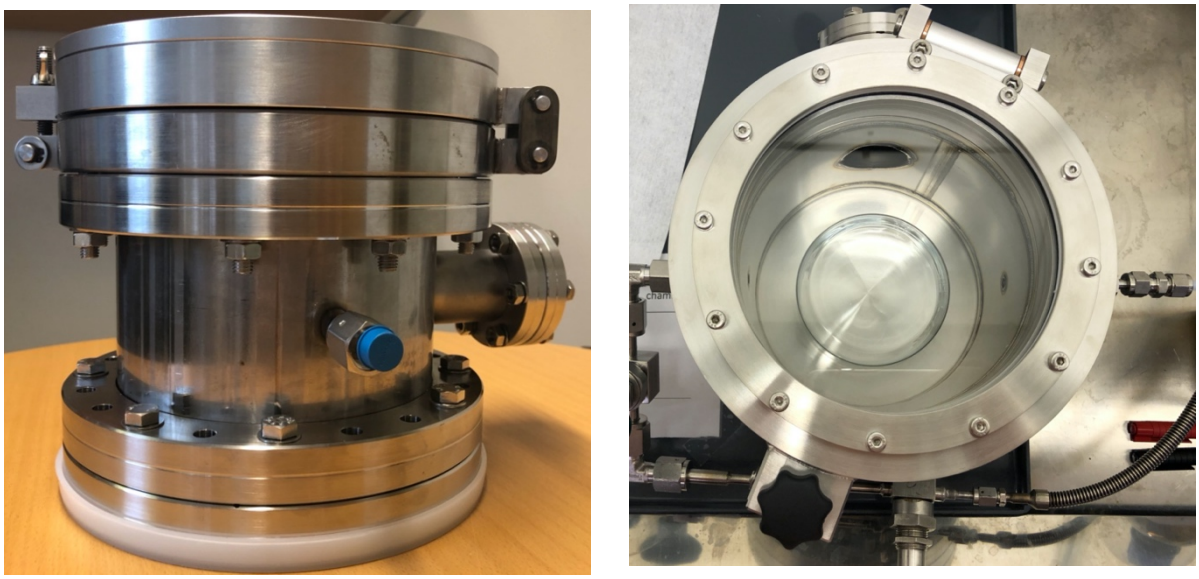

Figure 2-2: Images of the dynamic SVA chamber used in this project

Figure 2-2 are the images of the dSVA chamber built for this project. The body of the chamber is made of stainless steel, which has good tolerance to the solvents and a good thermal conductivity that is suitable for the temperature control during the annealing. Besides, it is safe for higher pressure that may be used in the experiments. The chamber is fabricated by combining an ISO straight connector with an access door with a viewport on top and a blank flange as the bottom. The viewport is made of quartz, which can have a quick check of the status of the annealing. The quartz window has a high transmittance which makes it favorable for the Filmetrics optical system (a spectral reflectance tool for thin film thickness and refractive index measurements) that will be connected to the chamber later for the in-situ measurements. The top flange can be easily opened to load and unload the samples. The diameter of the chamber is about 160 mm, and the height is about 110 mm. This is big enough for the 4-inch wafer and gives high evaporation rates of the solvents to create saturated stream of the carrier gas (N_2). Three feedthrough ports are added around the chamber, with two small ones as the inlet and the outlet of the solvent vapor in the symmetrical positions on the wall and a large one for the heater and its thermocouple.

There are copper O-rings between the connection of each part to prevent the leakage of the solvent and maintain desired pressure inside the chamber. No viton O-rings are used to prevent their possible damage by the solvents. The sample stage used in this project is a glass beaker with approximately 4 cm in height. This is the same height as the sample stage with a heater that is under construction now and will be assembled to the chamber later. All other materials used inside the chamber are resistant to the solvents used for the annealing.

2.2 Solvent Vapor Annealing Setup

After the well-controlled dynamic solvent vapor annealing chamber is assembled, an

effective dSVA setup based on the chamber is also formatted and used in this project.

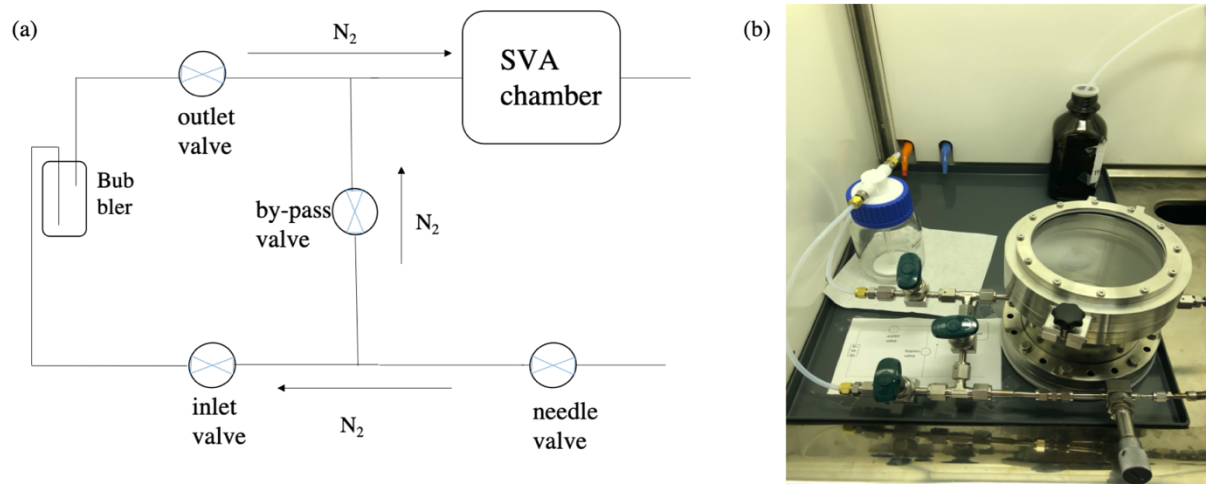

Figure 2-3 (a) Schematic of the dSVA setup; (b) image of the dSVA setup.

Figure 2-3 shows the schematic and the photo of the dSVA setup used in this project. The whole system is placed in the fume hood with sufficient ventilation. All tubings, coming to and from the chamber, have good resistance to the solvents used in the annealing process. Standard high purity N_2 is used as the source of the carrier gas. It is supplied by the house supply line on the wall in the lab and is controlled by the needle valve. The best way to control the flow rate is by using the mass flow controllers (MFCs), but due to some practical problems, MFCs could not be used in this project, unfortunately. The needle valve used here is similar to a micrometer with a scale mark on the screw. A calibration measurement between the scales on the needle valve and the real flow rate is made before the annealing experiments. The flow rates are measured by a flowmeter (Model 4140 D, Series 4100, TSI Inc., USA) connected after the inlet valve. The calibration results are shown in figure 2-4. The measurements are done both with and without the connection of the bubbler and got almost the same results. When doing the measurement with the bubbler, the bubbler is filled with water instead of solvents to prevent the contamination of the flowmeter.

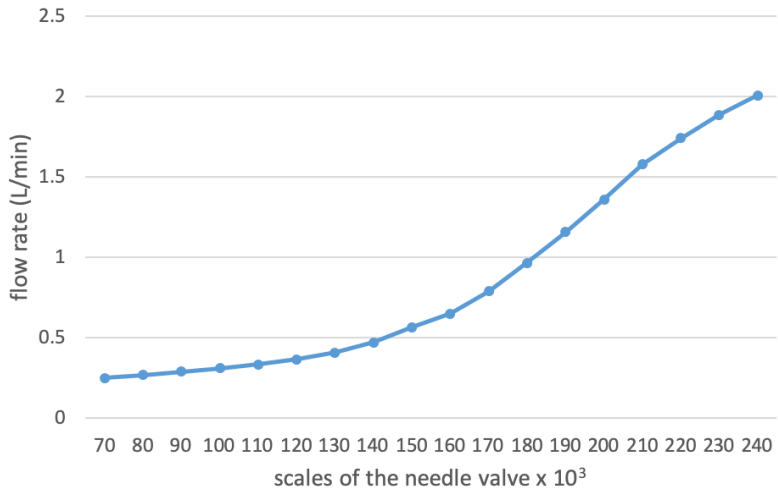

Figure 2-4 Calibration results between the scales on the needle valve and the real flow rate.

After the needle valve, there are two separate gas lines. One is the by-pass gas line, which used a flush of pure N_2 through the chamber, by-passing the bubbler. The pure N_2 is used to purge air from the chamber before annealing and flush the remaining solvents out of the chamber after annealing. This gas line is controlled by the by-pass valve shown in figure 2-3. The other gas line is the path of the N_2 travels through the bubbler and carries the solvents to the chamber. The N_2 bubble enters the solvent liquid, and with the increase of the interface area between N_2 bubble and solvent, the vapor pressure of the solvent in the new bubble increases. Therefore, the N_2 bubbles are completely saturated by the solvent when it pops up the bubbler, and the solvent is carried to the chamber with the gas stream. Figure 2-5 is the detailed image of the bubbler. The sparging head merged in the solvent liquid can help the bubbles disperse better. The inlet and outlet valve are the knob valves used to control the flow through the bubbler. By controlling the by-pass, inlet, and outlet valve, one can decide the path of the N_2 flow and change the different stages of the annealing.

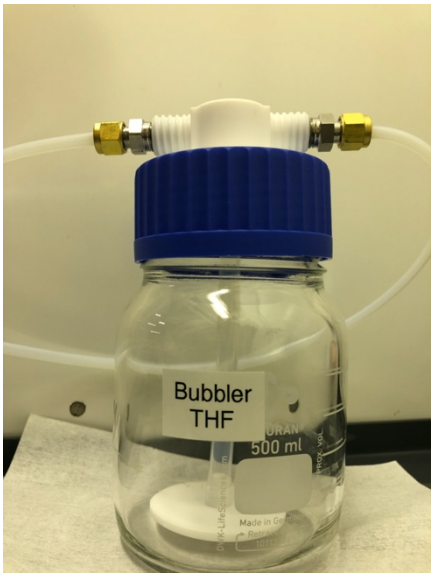

Figure 2-5 A detailed image of the bubbler

The solvent will interreact with the polymer films in the sealed chamber, and the gas is discharged from the chamber through the outlet. The outlet is connected to a waste bottle, which is filled with an appropriate amount of water to absorb the excess solvent. The waste bottle is not sealed, and the gas is exhausted through the ventilation.

2.3 Characterization Methods

2.3.1 Ellipsometry

Ellipsometry is a kind of optical measuring technique used to detect the thickness, optical constants (e.g. refractive index), and microstructure of thin films. Because of its high measurement accuracy, it is suitable for ultrathin film. The advantages such as non-contact with the sample, no damage to the sample, and no need of a vacuum, make the ellipsometry a very

attractive measurement instrument. The main principle of the ellipsometry is that the polarization state of the incident light is known, and the polarized light is reflected on the sample surface. By measuring the change of the polarization angle of the reflected light, the properties of the material can be calculated or fitted. After the measurement, the obtained data are used to analyze the optical constants, film thickness, and other parameters of interest.

The ellipsometry is used to measure the polymer thickness in this project, and it is a spectroscopic ellipsometer RC2 (Wollam Inc., USA). The angle of incidence in this ellipsometry is computer controlled and is generally in the range of 50º to 80º, and the wavelength is 200 to 1800 nm. In this project, the used incidence angle is 60º and 70º, and three positions are measured to obtain the thickness. The ellipsometry was used to accurately determine the thickness of the BCP film before and after the annealing experiments.

2.3.2 Atomic Force Microscopy (AFM)

Atomic force microscopy is an analytical instrument that can be used to study the surface structure of solid materials, including insulators. It analyzes the surface structure and properties of materials by detecting the weak atomic interaction between the sample surface and a micro force sensing element. When one end of the extremely force sensitive cantilever is fixed, the tip of the other end, which is close to the sample, will interact with the sample. The force will make the cantilever deflect or change its resonance frequency. When scanning the samples, the changes of the force distribution information can be obtained by sensors, so the surface morphology and structure information, as well as the surface roughness information, can be achieved with nanometer resolution. AFM is mainly composed of a cantilever with a needle tip, cantilever motion detection device, the feedback loop for monitoring its movement, computer-controlled image acquisition, and display and processing system. The motion of the cantilever can be detected by laser reflection. Once there is a short-range mutual repulsion force between the tip and the sample, it can be obtained by detecting the repulsion force and the surface atomic resolution image is formed. AFM has many advantages, such as that it provides real three-dimensional surface images. At the same time, AFM does not need any special treatment of the sample, such as copper plating or carbon deposition, which will cause irreversible damage to the sample. Thirdly, AFM can work well under atmospheric pressure or even in a wet environment. In this way, it can be used to study biological macromolecules and also living biological tissues, and it can observe non-conductive samples. However, the disadvantage of AFM is that the imaging range is too small, the speed is slow, and the influence of the probe is too considerable.

In this project, BCP films are characterized before and after SVA, using Bruker Dimension Icon (Bruker Inc., USA) atomic force microscope (AFM), operating in tapping mode. In the tapping mode, the cantilever oscillates just below its resonance frequency above the sample surface, and the tip of the needle only strikes the sample surface periodically and briefly. In this way, the lateral force generated when the tip contacts the sample is significantly reduced. Therefore, it is suitable for observing soft, fragile, or adhesive samples without

damaging their surfaces and can get high resolution at the same time. Below are some detailed parameters of AFM settings used in this project. The scan size is 500 nm with the aspect ratio of 1.00. The scan angle is 90º. The scan rate is set to 0.996 Hz and the cantilever scans 512 lines during one scan. To obtain better feedback, the integral and proportional gains are set as 0.4419 and 1.723, respectively, with a sufficiently small amplitude setpoint.

2.3.3 Optical Microscopy

Optical microscopy uses the magnifying imaging principle of a convex lens to magnify the small objects which cannot be distinguished by human eyes. It mainly increases the opening angle of the near small objects to the eyes to expand the object. The optical system of microscope mainly includes four parts: objective lens, eyepiece, reflector, and concentrator. An objective lens is the most crucial component to determine the performance of a microscope. The total magnification of the microscope is equal to the product of the magnification of the objective lens and the eyepiece. In this project, optical microscopy is used to have a quick check of the surface quality of BCP films after spin-coating and after annealing. Some macroscopic characteristics can also be obtained and can be used to make a general evaluation of the sample.

2.3.4 Summary of Characterization Methods

This part gives short introductions to the characterization methods used in this project. The most optimum thickness of the BCP film is that similar to the initial pattern distance in value, so the ellipsometry is essential for the project to get the proper thickness. For the detection of the surface organization, AFM, optical microscopy, and scanning electron microscopy (SEM) are the commonly used methods. SEM measurements provides a high-resolution, large-scale, and fast-gotten images of the sample. After the surface reconstruction in ethanol, which improves the image contrast, the sample can be used for SEM measurement later.

2.4 Summary

This chapter mainly discusses the first aim of this project: the design and building of a simple SVA chamber to provide a controllable environment for the annealing of BCP. It contains the design of the dynamic solvent vapor annealing chamber and the construction of the whole SVA setups as well as the detailed explanation of each part. Additionally, the characterization methodologies used in this project are introduced, with their fundamental theories and the applications in this project.

Chapter 3

Results of Time Controlled Solvent Vapor Annealing Process

3.1 Introduction

After the development of our well-controlled dynamic solvent vapor annealing setup, the next vital step is investigating the proper SVA parameters to optimize the system and get the polymer morphology we want, which is the hexagonally oriented vertical cylinder structure. The first parameter investigated in this project is the annealing time, which will be discussed in this chapter in detail. A complete solvent vapor annealing process can be divided into two stages: the polymer swelling stage due to the diffusion of solvent in the film that results in increase of film thickness, and the drying stage to evaporate the solvent and restore to the initial thickness. The swelling will continue until the chemical potential of the solvent in the film equals that of the solvent in the vapor phase (6). In this chapter, the exposure time of the BCP film to solvent is changed to find out when the film can reach the steady-state and form a well-organized structure. The drying time is set to be constant for all the experiments.

The final thin film assembly is also susceptible to exact SVA conditions, such as the temperature, solvent vapor flow rate, vapor pressure, and solvent selectivity. In order to get a better result of the relationship between the annealing time and the surface assembly, all the other parameters are set to be unchanged for all the experiments. According to the calibration results that were described in the previous chapter, the lowest flow rate is chosen for the annealing, which is 0.25 L/min. If the flow rate is too high, the solvent will pass through the entire gas line at a high speed and make it difficult to reach the saturation state inside the chamber. Furthermore, according to the phenomenon that happened during the calibration measurements, for a high flow rate, condensation may occur in the chamber, which is not desirable during the annealing process. The condensation was due to an intensive evaporation in the bubbler at a high flow rate, and this causes the temperature to decrease. A heating system should be induced to prevent this condensation of the solvent, which could not be implemented for this project currently. Therefore, a small flow rate is chosen for this project. The annealing is operated at room temperature. Assuming the volume of the solvent carried by N_2 bubbles, which is about 1 ml/min, is constant, and the equilibrium pressure in the chamber can be reached quickly. With the constant N_2 flow rate, the vapor pressure inside the chamber is also constant. The selection of the solvent is also foremost for the annealing process. In this project, for the initial experiments, tetrahydrofuran (THF) is used, which has some selectivity of polystyrene. Besides, THF has a high evaporation pressure and evaporates fast from a solution, which has earlier been simulated to promote vertical cylinders (18).

3.2 Experiment

3.2.1 Sample Preparation

Poly(Styrene)-block-Poly(4-Vinylpyridine) (PS-*b*-P4VP), with a molecular weight of 50k Poly(Styrene) and 17k Poly(4-Vinylpyridine), and a polydispersity of 1.15 from Polymer Source Inc. (Canada), was then dissolved, to a 0.625 wt% solution, in a Tetrahydrofuran: Toluene mixture in a 4:1 volume ratio. In order to make polymer dissolve better and produce a uniform solution, the mixture was first put in the ultrasonic bath at 40ºC for 40 min and let stand overnight at room temperature. The mixture of the polymer was spin-coated on the 1.5x1.5 cm^2 Si substrates. The Si substrate was first cleaned by acetone and isopropanol (IPA) with an ultra-sonic bath for 3 min individually. Then the substrates were pre-baked on a hotplate at 200°C for 10 minutes for surface dehydration and to improve adhesion to the polymer. After that, the samples were let to cool down for 90 seconds. The PS-*b*-P4VP films were spin-coated on Si substrates at 5000 rpm speed and baked on a hotplate at 120°C for 3 min to finish the sample preparation. The thickness of the BCP films is measured by the ellipsometry and is found to be in the range of 50 to 57 nm. An optical microscope is used to make a quick check of the spin-coating quality. The sample is also characterized by AFM to obtain the initial surface morphology.

3.2.2 Solvent Vapor Annealing

Solvent vapor annealing is performed in the dynamic SVA system placed in a fume hood using tetrahydrofuran (THF) as the solvent. The detailed SVA procedures are mentioned below. The experiment started with cleaning the chamber and the sample stage with IPA. After that, the N_2 supply on the wall and the by-pass valve were opened to create a massive flow to dry the chamber. After the chamber was completely dried, the valve on the gas line was wholly closed with no leak of N_2.

After loading the sample, the annealing process is performed. Firstly, only the by-pass valve was on for 5 min with a flow rate of 2 L/min to purge the chamber. Then the flow rate of 0.25 L/min used for annealing was set by changing the needle valve with the inlet valve and outlet valve on and by-pass valve closed. Then the system was left for the SVA process with a desired annealing time. When the annealing process is finished, the by-pass valve was switched on and the inlet and outlet valve set off to let pure N_2 flush all the solvent and perform the drying stage for 10 min. After unloading of the sample, it is characterized by AFM to obtain the surface structures.

3.3 Results and Discussion

The annealing time varies from 15 min to 2 h in this project. All samples are annealed at room temperature with a flow rate of 0.25 L/min. Figure 3-1 below shows the AFM results before and after annealing.

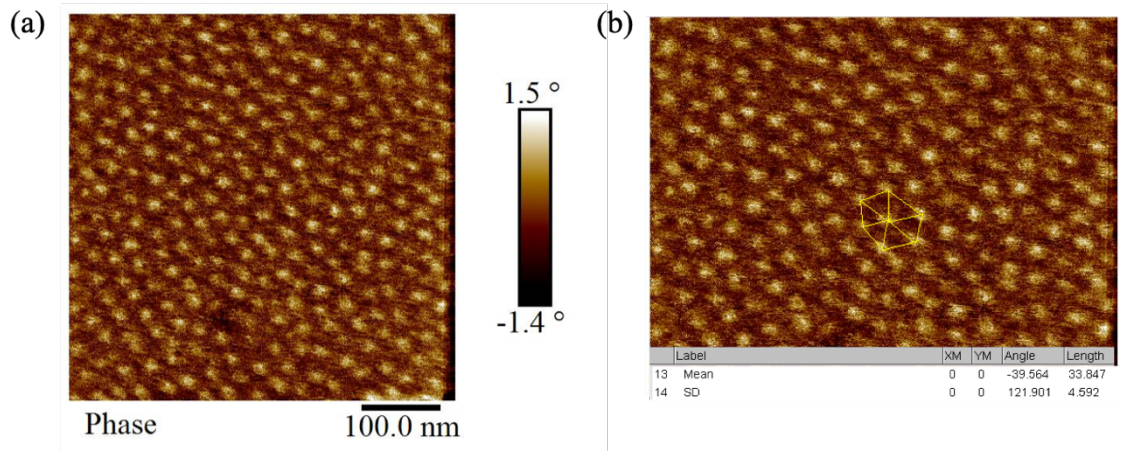

Figure 3-1 AFM results of the BCP films before annealing. (a) The result in phase mode; (b) The initial pitch measured by ImageJ

Figure 3-1 (a) shows the AFM result of a BCP film before annealing. From it, we can find that the polymers already have some self-organization after the baking in the last step of the spin-coating procedure. The brighter dots in the figure are P4VP blocks, and they are embedded in polystyrene matrix. As expected, P4VP here forms the cylinders, which are perpendicular to the substrate. Although it has the vertical cylinder structure that is preferred, the domain structure is kind of chaotic. The well-organized structure is the hexagonally packed cylinders. The thickness of the BCP film shown here is 50.6 nm. The thickness of the BCP film is mainly determined by the molecular weight of each polymer and the polymer concentration of the solution used for spin-coating. These two factors are fixed, so we got almost the same thick BCP films, and the influence of thickness is not taken into account. Though the thickness of the BCP film varies a little, from 50 to 57 nm, due to the different amounts of liquid dropped on the sample during spin-coating, the detected morphology is similar. To obtain a more representative data, the AFM scans were performed at three different positions on each sample: one was in the center of the sample, others were 2.5 mm in x- and y-directions from the center, respectively. All morphology of the same sample is identical, and this shows the potential in the large-area application.

Figure 3-1 (b) shows the analyzed results using ImageJ software. One of the most important parameters is a pitch of the BCP film, which is the distance between neighboring dot centers. The most hexagonal-liked regime is found, and the distance between every neighboring dot in the honeycomb cell is measured to obtain the average pitch of the pattern. The measured mean value of this sample is 33.8 nm. The pitch of different samples varies not too much, from 32 to 35 nm approximately.

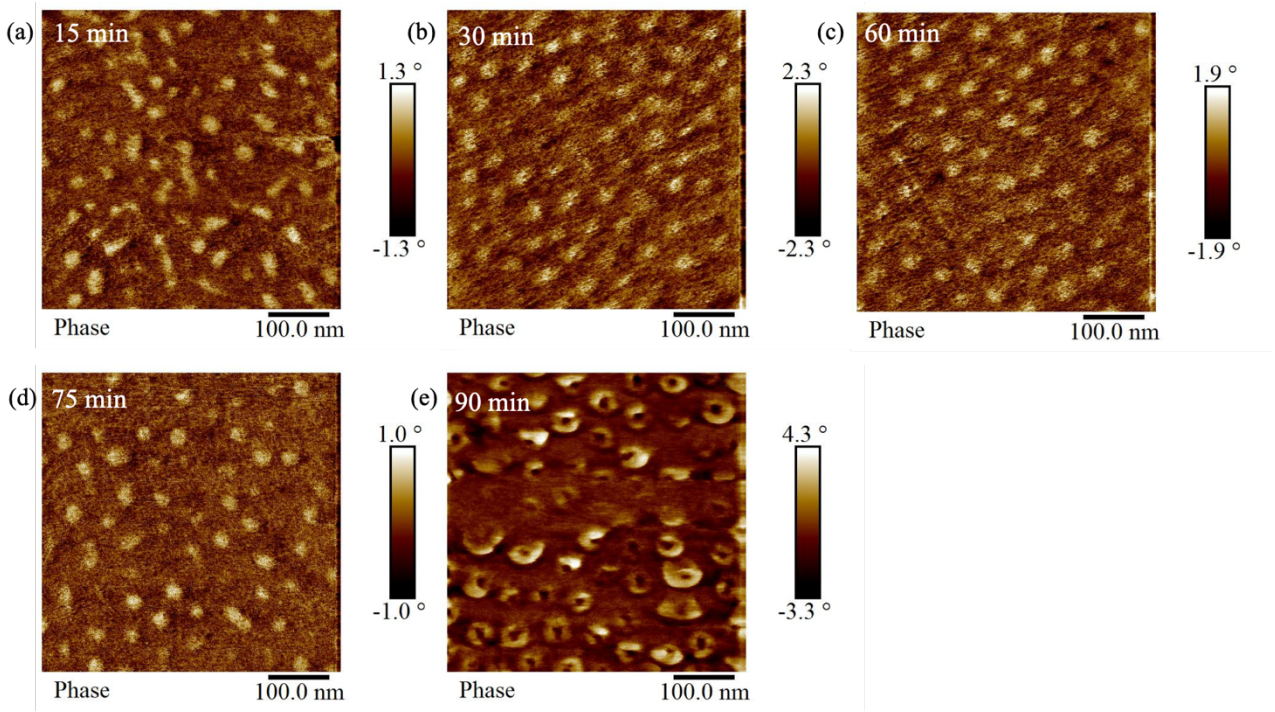

Figure 3-2 AFM results in phase mode of samples after annealing with different annealing times. (a)-(e) are samples after 15, 30, 60, 75 and 90 min annealing respectively.

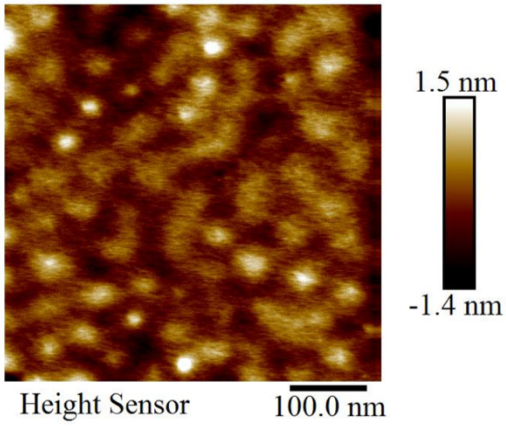

Figure 3-3 AFM result in height mode for sample after 120 min annealing.

Figures 3-2 and 3-3 show the AFM results of samples after annealing with different annealing times. The difference and transition in morphology with different annealing time can easily be seen. Figure (a) is the result after 15 min annealing. From this image, we can conclude that the solvent swollen state is already started after 15 minutes. The domain shape changes and some polymer movements appear in this figure. During the polymer swelling, the polymer concentration and the volume fraction of the components changes that results in the end, in changing of the domain shape (7). The solvent improves the polymer mobility and helps the polymer to overcome its potential barrier, which makes it be able to transform to its equilibrium structures. However, the poorly organized P4VP microdomains indicate the time is not sufficient enough for P4VP to move freely and kinetically reach the equilibrium state (19). Figure 3-2(b) is the result after 30 min annealing, and we can see the vertical cylinder patterns.

The pitch increase to about 55 nm is also visible in the figure. However, the cylinders are not well hexagonally packed after 30 minutes, which means the self-diffusivity is still low for this annealing time, so longer annealing time is required to reach the equilibrium state. For results obtained after 60 minutes annealing, which is shown in (c), it is obvious that the vertical cylinder patterns remain, and it is easier to find the hexagonal structures. The details of the hexagonal structures are shown in figure 3-4. The pitch of this sample increases, and the sizes of the cylinders increase as well, with an average diameter of P4VP blocks of 17 nm. Therefore, one can conclude that after 1 h annealing the most preferred organization among all the experiments is obtained.

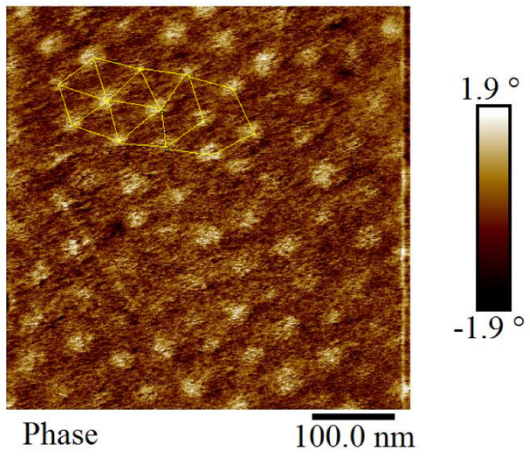

Figure 3-4 The details of the hexagonal structures of sample annealed for 1 h.

For SVA time of longer than 1 h, which is shown in figure 3-2(d)(e) and figure 3-3 the self-organization degenerates. This may be because of the increased difficulty of overcoming the polymer-surface interaction due to the high degree of swelling (20). For the sample annealed for 1h 30 min, figure 3-2(e) shows some pore-opening phenomena, which indicates the high defect density in terms of the morphology heterogeneity (8). For the sample annealed for 2 h, the height mode of the AFM result is used because of the little information provided by the phase mode. Here a mix of vertical and parallel cylinders are formed and the preferred organization is lost.

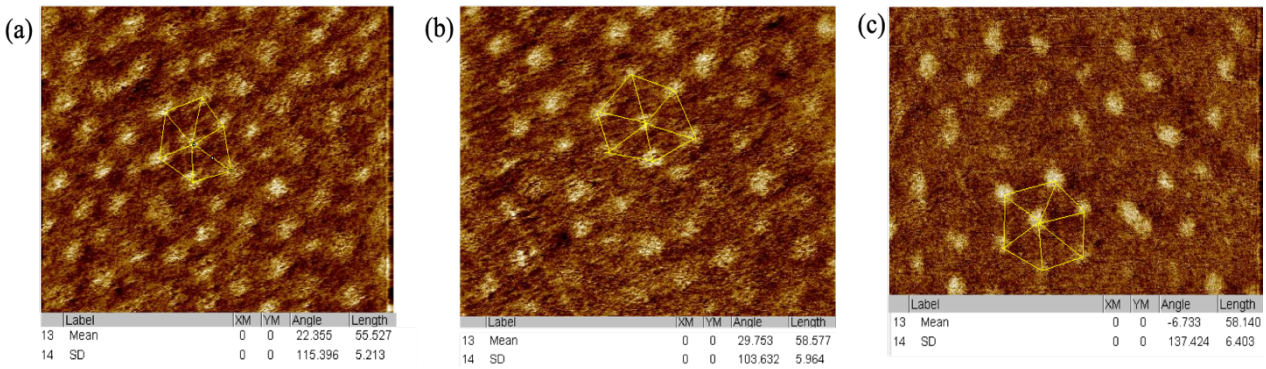

Figure 3-5 The pitch measurement results. (a)-(c) are results for samples after 30, 60, and 75 min annealing respectively.

The pitch results in figure 3-5 are calculated in the same way as the initial pitch. After 30 minutes annealing, the pitch increases from 33.9 nm to 55.5 nm, which shows a big difference. After 1 h annealing, the pattern periodicity reaches 58 nm and stops any further increase. The pitch of the BCP film is determined by the Flory–Huggins interaction parameter χ and degree of polymerization N. Both of these are related to the molecular weight of each polymer and the volume fraction, which are all fixed in this experiment. Therefore, although the block copolymer has the vertical cylinder morphology just after spin-coating, it does not reach its equilibrium pitch after the deposition because of the substrate-polymer interaction. By increasing the annealing time, the solvent front gradually diffuses from the vapor interface through to the substrate and reorganized to the desired state during the swollen stage. The equilibrium pitch of this kind of block copolymer system we used is about 58 nm, which is comparable to the initial thickness of BCP films and agrees with the results gotten by previous sSVA with two kinds of solvents. Figure 3-6 shows the relationship between the pitch and the annealing time, where one can see that the pitch reaches its plateau after about 60 min annealing.

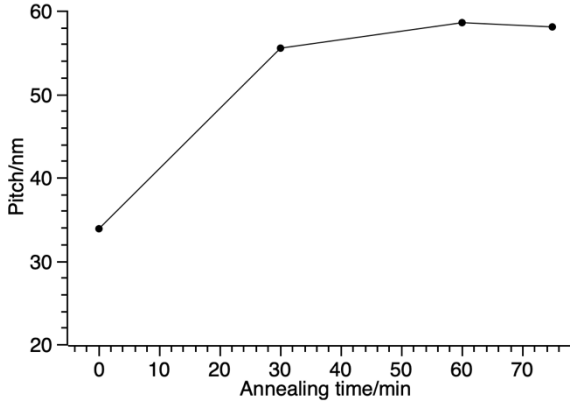

Figure 3-6 The relationship between the pitch and the annealing time.

To check whether the dynamic solvent vapor chamber fulfills our targets and shows improvement in the solvent vapor annealing process, a reference sample is annealed in the sSVA setup. The solvent used here is 10 ml THF liquid in the larger beaker and it is annealed for 4 h at room temperature. The AFM result after annealing is shown in figure 3-7.

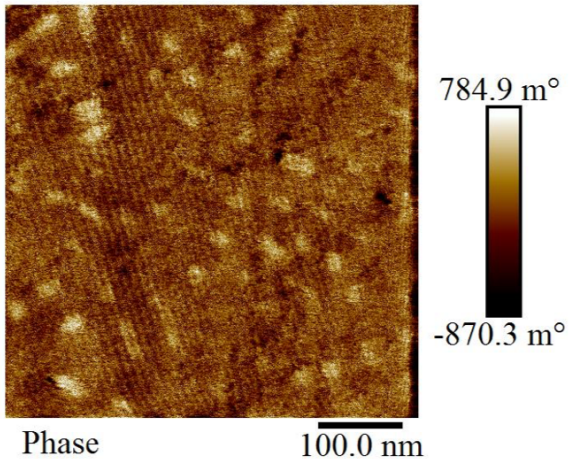

Figure 3-7 AFM result in phase mode of the reference sample.

For this reference sample, there is no well-ordered pattern after annealing, and it shows the similarity to figure 3-2(a), which is the result of 15 min annealing in the dynamic chamber. This means the annealing time is greatly reduced by using the dynamic SVA chamber. The dynamic SVA system takes advantage of steady-state vapor flows formed in it, while the sSVA system relies on a more equilibrium like vapor condition (5). Besides, the saturate pressure inside the chamber is easier to reach compared to a small partially closed container. These two parameters contribute to a faster annealing process in the dSVA setup.

3.4 Summary

In this chapter we investigated the effects of annealing time in dSVA chamber on re-arrangement of the PS-*b*-P4VP BCP films. By fixing other SVA conditions, such as the temperature, solvent vapor flow rate, vapor pressure, and solvent selectivity, good results indicating a relationship between the annealing time and the surface assembly are obtained. For this SVA system, which uses PS-*b*-P4VP block copolymer and THF as the annealing solvent, the best organization for the 50-57 nm thick polymer is obtained after 1h annealing, which has a hexagonally oriented vertical cylinder structure with a 58 nm equilibrium pitch. By changing the annealing time, different steps in SVA process are also obtained, which helps us to get a profound understanding of the kinetics of the self-organization process.

Chapter 4

Results of Thickness Controlled Solvent Vapor Annealing Process

4.1 Introduction

Block copolymer film thickness is also a critical parameter affecting the final polymer organization after annealing. The thickness should be comparable to the natural domain periodicity of the block polymer for formation of well-ordered vertical cylinders structure. As it is shown in the previous chapter, the thickness obtained after spin-coating was about 50-57 nm, while the initial pitch is around 32-35 nm. Therefore, we considered to reduce the polymer thickness to a value close to the initial pitch to see the its influence on the final polymer organization after annealing. The results of the thickness controlled solvent vapor annealing process are discussed in this chapter.

By decreasing the thickness of the film, the amount of total polymer coated on the substrate is decreased as well, and emphasize the thermodynamic and dynamic importance of the two interfaces, which are with the substrate and the free surface. A thinner layer can also avoid the multilayer fraction after spin-coating (21).

4.2 Experiment

The Poly(Styrene)-*block*-Poly(4-Vinylpyridine) used here is the same as the previous one in the previous chapter. There are two ways to change the thickness during spin-coating, one is to change the rotating speed in the spin-coating program, and the other is to change the concentration of the polymer solution used for spin-coating. However, the first method is not so efficient and does not have a reasonable control of the thickness. The method of changing the thickness used in this chapter is changing the solution concentration.

The polymer was still dissolved in a Tetrahydrofuran: Toluene mixture in a 4:1 volume ratio and dissolved in the same way. Three different concentrations are used in this chapter: 0.50 wt%, 0.40 wt%, and 0.30 wt%. The speed of spin-coating was the same, which was 5000 rpm. After checking the samples by ellipsometry, the following film thicknesses are obtained: around 43 nm, 32 nm, and 27 nm by using the concentration mentioned above, respectively. These thicknesses vary ideally around the value of the initial pitch measured earlier.

The annealing was done in the same dynamic SVA system with THF as the solvent and 0.25 L/min as the N_2 flow rate. Samples are still annealed in room temperature, and all other conditions and procedures are the same as described in chapter 3. The annealing times chosen for this chapter are 30 min and 60 min when we can find a considerable well-organized structure in previous experiments. Three samples with three different thicknesses mentioned above are annealed together for one specific annealing time. This is used to reduce other variables that

may appear in the experiment and have a better investigation of the thickness influence.

4.3 Results and Discussion

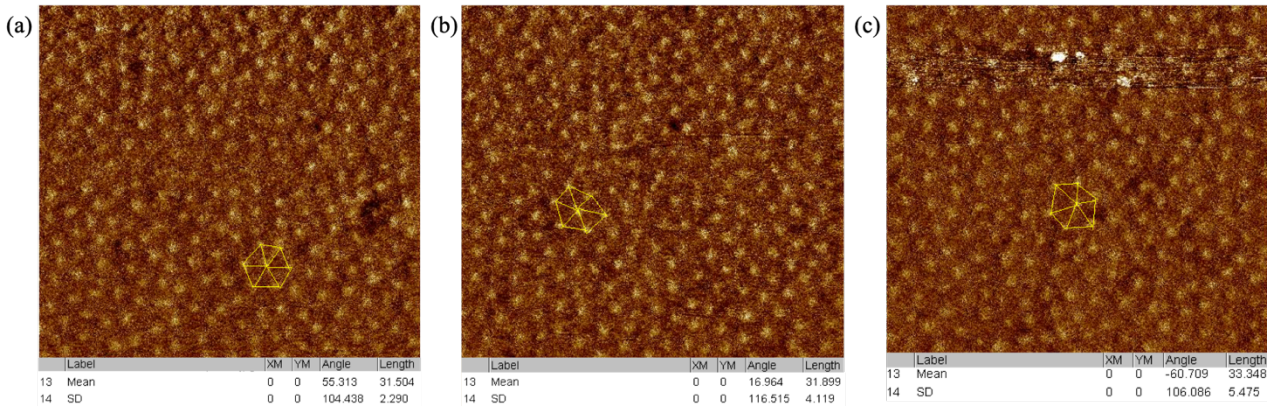

Figure 4-1 AFM results and measured the pitch of samples with different thicknesses before annealing. (a) the result of 43 nm film; (b) the result of 32 nm film; (c) the result of 27 nm film.

Figure 4-1 shows AFM results and measured the pitch of samples with different thicknesses before annealing. They all have similar vertical cylinder patterns and almost the same pitch. However, they are all more challenging to find the hexagonal structures compared to figure 3-1. The initial pitch is rather close to the result in chapter 3. This means the thickness has very little influence on the initial morphology of BCP films after spin-coating.

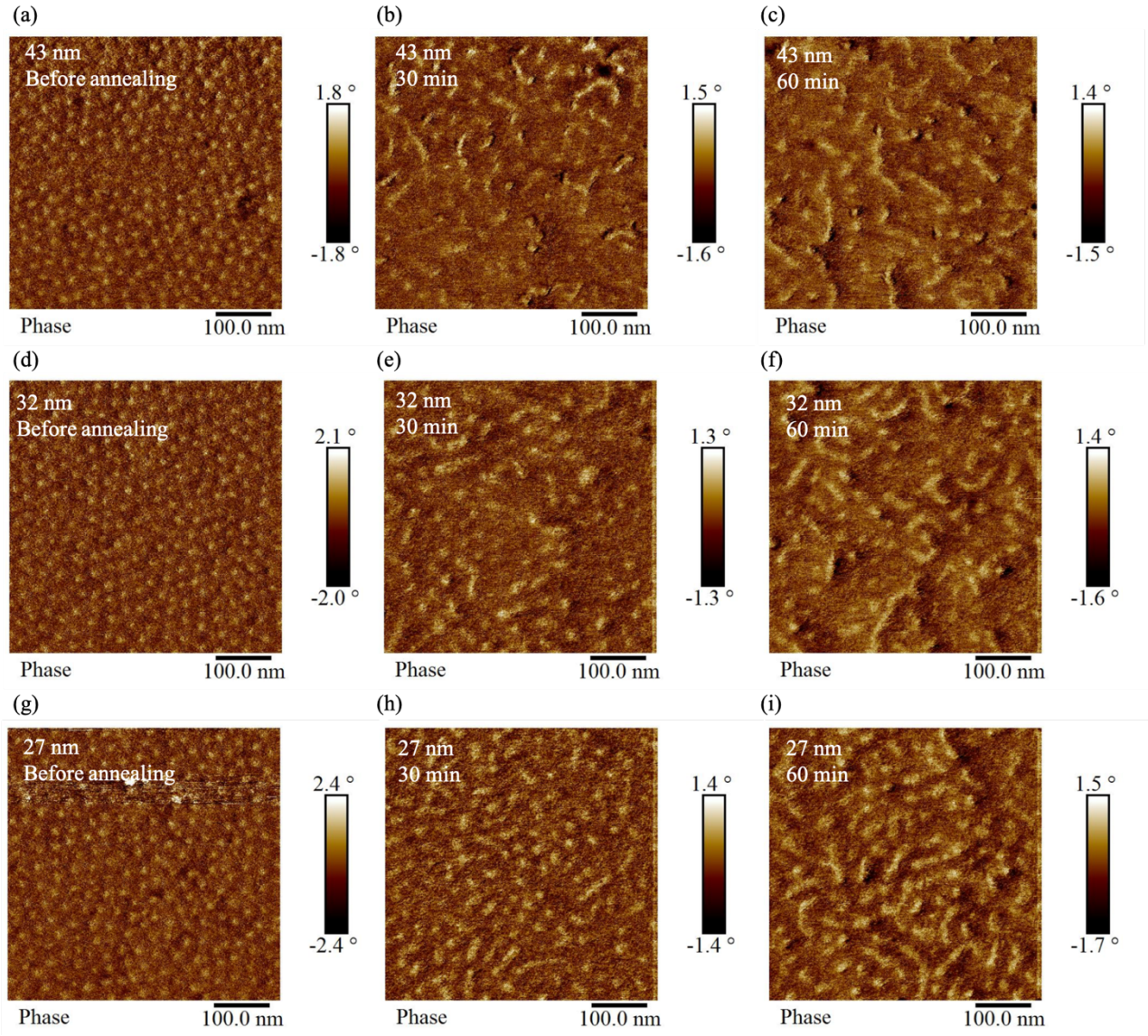

Figure 4-2 AFM results in phase mode of samples with different thickness after annealing with different annealing time. (a)-(c) are 43 nm thick samples; (d)-(f) are 32 nm thick samples; (g)-(h) are 27 nm thick samples. (a)(d)(g) are results before annealing; (b)(e)(h) are results after 30 min annealing; (c)(f)(i) are results after 60 min annealing.

Figure 4-2 shows AFM results of samples with different thickness after annealing with different annealing time. BCP films lose the self-organization after annealing no matter the thickness and annealing time. They all have a mixed structure with vertical and parallel cylinders after annealing, and the ratio and lengths of parallel cylinders increases over time.

The initial layer thickness is highly relevant to the BCP confinement between the substrate and top interface, which influences the morphology. By changing the film thickness, the distance between the free surface and the chamber bottom also changes, which may result in varying vapor pressure conditions and thus different morphology. For thinner BCP film, the diffusion time for the solvent front transform from the vapor interface through to the substrate

is shortened, and thus accelerate the annealing process. The results of thinner layers may be similar to those of 50 nm thick BCP films with more than 2 h annealing experiments that were not carried out in this project. They may reach their equilibrium states in annealing time shorter than 30 min, which is not performed due to the lack of time. This also proves that BCP films do not reach their equilibrium states after spin-coating, and 32 nm pitch is not the equilibrium result. Another explanation is that these thinner samples simply are too thin to self-assemble into vertical cylinders over time.

4.4 Summary

This chapter mainly discusses the relationship between initial polymer thickness and the final polymer morphology after annealing. Three different thicknesses: around 43 nm, 32 nm, and 27 nm are obtained by changing the concentration of the polymer solution. After using the same annealing condition, an accelerated annealing process is observed because of the shorter diffusion time for the solvent front transform from the vapor interface through to the substrate. The equilibrium state should be reached sometime before 30 minutes annealing.

Chapter 5

Conclusion and Outlook

5.1 Conclusion

Self-assembled block copolymers thin films provide an inexpensive and straightforward approach to nano-size patterning and can be used in lithography and with other nano fabrication methods. However, the self-assembled structures may not be well-organized or not be the preferred structure for further use. In order to control the self-assembly, an additional annealing step is required. Very often, the annealing is performed in a suitable vapor atmosphere, using so-called solvent vapor annealing. This thesis starts with the introduction to the block copolymer system and annealing methods. The two main parts of this project included (1) design and building of a dynamic solvent vapor annealing chamber to provide a controllable environment for the annealing of BCPs and (2) investigation of optimum annealing conditions in the dynamic solvent vapor annealing setups and study of self-assembly kinetics of PS-*b*-P4VP films on Si substrate.

In the project, a dynamic solvent vapor annealing chamber, which provides a controllable environment for the annealing of the BCPs, is successfully built. The primary purpose of this device is to create a stable solvent vapor atmosphere with one or more solvents for the thin polymer film placed in it. This chamber that can maintain constant humidity, temperature, and the solvent vapor evaporating rate during the annealing, is successfully tested. This dSVA system takes advantage of steady state vapor flows formed in it, and a sufficient acceleration in the annealing process is observed. Furthermore, the chamber is also designed to have good control of the pressure and temperature during the annealing and available for in-situ measurements during the annealing process.

After the development of this well-controlled dynamic solvent vapor annealing setup, the next vital step is investigating the proper SVA parameters to optimize the system and obtain hexagonally oriented vertical cylinder structure. The first variable parameter is the annealing time. By fixing other SVA conditions, such as the temperature, solvent vapor flow rate, vapor pressure, and solvent selectivity, the relationship between the annealing time and the surface assembly is obtained. For this SVA system, which uses PS-*b*-P4VP block copolymer and THF as the annealing solvent, the best organization for the 50-57 nm thick polymer is obtained after 1h annealing, which has a hexagonally oriented vertical cylinder structure with a 58 nm equilibrium pitch. By changing the annealing time, different steps in SVA process are also obtained, which helps us to get some understanding of the kinetics of the self-organization process.

The initial polymer thickness is another vital parameter affecting the final polymer organization after annealing. Due to the difference between the initial pitch and polymer

thickness, the second variable parameter is the BCP film thickness. This is obtained by changing the concentration of the polymer solution. Three different thicknesses are investigated: around 43 nm, 32 nm, and 27 nm. After using the same annealing condition, an accelerated annealing process is observed because of the shorter diffusion time for the solvent front transform from the vapor interface through to the substrate. The equilibrium state should be reached sometime before 30 minutes annealing.

5.2 Outlook

Due to the delay caused by the coronavirus epidemics, the goal of this project is not completely reached. Some other functions can be added to the dynamic solvent vapor annealing chamber, such as the temperature controlling system and MFCs for the control of the vapor flow rate. We have already received the heater for the sample stage and is under construction with the sample stage. In order to form a complete heating system, some tape heater can also be added to heat the gas lines, bubbler, and chamber walls. By using the MFCs, better control of the vapor flow rate can be reached and makes it possible to monitor the flow rate and pressure during annealing. The initial design of the SVA setups is for two or three kinds of annealing solvent that can be controlled independently. However, the current setup is suitable for only one solvent. The gas lines can also be changed to achieve the initial design. Figure 5-1 shows the AFM results of the polymer after 4 h annealing with THF: Methanol mixture in a 9:1 volume ratio and a total volume of 10 ml using the sSVA beaker. The well-organized hexagonally oriented vertical cylinder structure is formed, which shows the advantage of using two kinds of solvent with different selectivity to the polymer to improve annealing results.

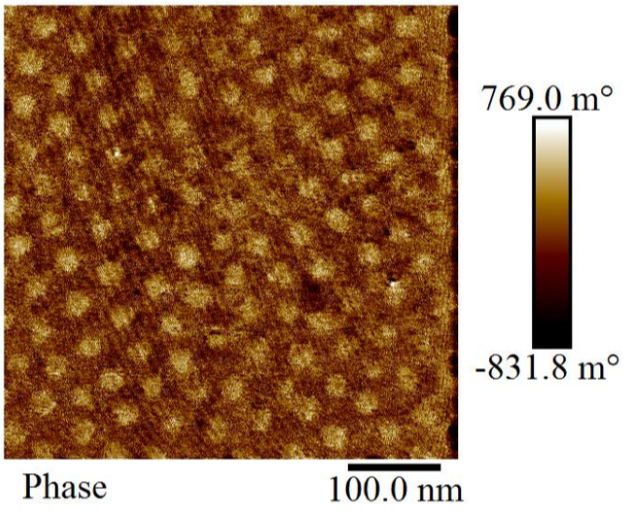

Figure 5-1 AFM results of a reference sample annealed with THF and Methanol.

Some other annealing parameters can also be changed to investigate an optimized setup for the dynamic solvent vapor annealing system, such as the temperature, flow rate, and solvent selection. These will also be helpful for the study of the kinetics of the self-organization process of the BCP films. An in-situ measurement, such as the Filmetrics optical system, can also be assembled to the SVA system. The Filmetrics setup can measure the thickness change during

the swollen state and drying state, which shows considerable assistance in investigating the dynamic mechanism behind the solvent vapor annealing process.

Due to the low contrast and the charge phenomena at the surface of the BCPs, SEM is not used as a characterization method in this project. However, SEM provides high-resolution, large-scale, and fast-gotten images of the sample, and it is a commonly used method for SVA analysis. After the surface reconstruction in ethanol or ALD treatment, the sample can be used to enhance the contrast for SEM measurements. This is also a direction for the future work.

References

1. Cui Z. Nanofabrication Principles, Capabilities and Limits2017.
2. Bratton D, Yang D, Dai J, Ober CK. Recent progress in high resolution lithography. Polymers for Advanced Technologies. 2006;17(2):94-103.
3. Morris MA. Directed self-assembly of block copolymers for nanocircuitry fabrication. Microelectronic Engineering. 2015;132:207-17.
4. Bates FS. Block Copolymer Thermodynamics: Theory and Experiment. Phys Chem 1990;41:33.
5. Gotrik KW. Flow Controlled Solvent Vapor Annealing of Block Copolymers for Lithographic Applications: Massachusetts University; 2013.
6. Sinturel C, Vayer M, Morris M, Hillmyer MA. Solvent Vapor Annealing of Block Polymer Thin Films. Macromolecules. 2013;46(14):5399-415.
7. Gu X. Self-Assembly of Block Copolymers by Solvent Vapor Annealing, Mechanism and Lithographic Applications: University of Massachusetts - Amherst; 2014.
8. Lundy R, Flynn SP, Cummins C, Kelleher SM, Collins MN, Dalton E, et al. Controlled solvent vapor annealing of a high chi block copolymer thin film. Phys Chem Chem Phys. 2017;19(4):2805-15.
9. Cummins C, Ghoshal T, Holmes JD, Morris MA. Strategies for Inorganic Incorporation using Neat Block Copolymer Thin Films for Etch Mask Function and Nanotechnological Application. Adv Mater. 2016;28(27):5586-618.
10. Memisevic E, Svensson J, Lind E, Wernersson L-E. Vertical Nanowire TFETs With Channel Diameter Down to 10 nm and Point SMIN of 35 mV/Decade. IEEE Electron Device Letters. 2018;39(7):1089-91.
11. Bjork MT, Ohlsson BJ, Sass T, Persson AI, Thelander C, Magnusson MH, et al. One-dimensional Steeplechase for Electrons Realized. Nano Letters. 2002;2:3.
12. Nelson G, Drapes CS, Grant MA, Gnabasik R, Wong J, Baruth A. High-Precision Solvent Vapor Annealing for Block Copolymer Thin Films. Micromachines (Basel). 2018;9(6).
13. O'Driscoll S, Demirel G, Farrell RA, Fitzgerald TG, O'Mahony C, Holmes JD, et al. The morphology and structure of PS-b-P4VP block copolymer films by solvent annealing: effect of the solvent parameter. Polymers for Advanced Technologies. 2011;22(6):915-23.
14. Jung A, Rangou S, Abetz C, Filiz V, Abetz V. Structure Formation of Integral Asymmetric Composite Membranes of Polystyrene-block-Poly(2-vinylpyridine) on a Nonwoven. Macromolecular Materials and Engineering. 2012;297(8):790-8.
15. Bhoje Gowd E, Nandan B, Vyas MK, Bigall NC, Eychmuller A, Schlorb H, et al. Highly ordered palladium nanodots and nanowires from switchable block copolymer thin films. Nanotechnology. 2009;20(41):415302.
16. Park S, Wang J, Chen W, Russel TP. Solvent-Induced Transition from Micelles in Solution to Cylindrical Microdomains in Diblock Copolymer Thin Films. Macromolecules. 2007;40:5.
17. Wang Y, Narita C, Xu X, Honma H, Himeda Y, Yamada K. Controlling the ordered transition of PS-b-P4VP block copolymer ultrathin films by solvent annealing. Materials

Chemistry and Physics. 2020;239.
18. Hao J, Wang Z, Wang Z, Yin Y, Jiang R, Li B, et al. Self-Assembly in Block Copolymer Thin Films upon Solvent Evaporation: A Simulation Study. Macromolecules. 2017;50(11):4384-96.
19. Rasappa S, Hulkkonen H, Schulte L, Ndoni S, Reuna J, Salminen T, et al. High molecular weight block copolymer lithography for nanofabrication of hard mask and photonic nanostructures. J Colloid Interface Sci. 2019;534:420-9.
20. Hulkkonen H, Salminen T, Niemi T. Automated solvent vapor annealing with nanometer scale control of film swelling for block copolymer thin films. Soft Matter. 2019;15(39):7909-17.
21. Yang Q, Loos K. Perpendicular Structure Formation of Block Copolymer Thin Films during Thermal Solvent Vapor Annealing: Solvent and Thickness Effects. Polymers (Basel). 2017;9(10).

Acknowledgment

I would like to acknowledge several people who contributed to this thesis. I would like to thank my supervisor Ivan Maximov for his guidance throughout the thesis process. I would like to thank Anette Löfstrand for all the hours in the lab and her invaluable help through the project. I would like to thank Bengt Meuller for his work to build the SVA chamber. I would like to thank all of the related staff in the Lund Nano Lab for the support and instructions to the tools. Also, I would like to thank all the friends I made in Lund for the accompany during these two years. Finally, I would like to thank my parents for their support and dedication even they are in China far from me.